Universal Journal of Mechanical Engineering 10(1): 1-12, 2022
DOI: 10.13189/ujme.2022.100101 http://www.hrpub.org

Comfort Assessment in Railway Vehicles by an Optimal Identification of Transfer Function

Massimo Cavacece

Department of Civil and Mechanical Engineering, University of Cassino and Southern Lazio, Italy

Received December 11, 2021; Revised March 20, 2022; Accepted April 15, 2022

Cite This Paper in the following Citation Styles

***(a)**: [1] Massimo Cavacece, "Comfort Assessment in Railway Vehicles by an Optimal Identification of Transfer Function," Universal Journal of Mechanical Engineering, Vol.10, No.1, pp. 1-12, 2022. DOI: 10.13189/ujme.2022.100101*

***(b)**: Massimo Cavacece, (2022). Comfort Assessment in Railway Vehicles by an Optimal Identification of Transfer Function. Universal Journal of Mechanical Engineering, 10(1), 1-12, DOI: 10.13189/ujme.2022.100101*

Abstract `Purpose` This research proposes a multi–input multi–output (MIMO) model, based on a data–driven approach, to assess passenger vibration comfort on rail vehicles. The MIMO model represents the mathematical relationship between input and output variables that contains modal properties and vibration transmission. An optimization algorithm estimates the frequency response functions at the interface seat–passenger of the trains.
`Methods` The MIMO model evaluated the frequency response functions along x–, y– and z– axis. Multivariate analysis considered the calculation of the partial coherence functions, the cross–correlation functions, and the Anderson–Darling nonparametric test.
`Results` This research considered the acceleration measurements on two Trains, one Tramway, and one Underground. This research developed accelerations analyses in the time domain; the transmissibility of accelerations in the frequency domain. The measuring points were on the seat base and the interface seat–passenger of the trains. The frequency response data, obtained experimentally according to x– y– and z–axis, generated a multi–input and multi–output frequency response model. This research is based on experimental investigations and statistical tests. The calculation of partial coherence evaluated the percentage of spectrum output due to a specific (conditional) input. The partial coherences assess the energy contribution of each input to the output. The cross–correlation test showed the phase between input and output accelerations. The Anderson–Darling test showed the provenance of the data sample from a population with a specific distribution. Anderson–Darling's nonparametric test attaches weight to tails.
`Conclusions` The seats of the trains were exposed to complex vibrations according to the three directions x, y, and z. The three inputs are linear accelerations along the vertical, lateral, and forward direction of the seat base. If the accelerations on the seat base represented the inputs to the MIMO model, the accelerations acquired at the passenger–seat interface represented the output of the MIMO model.

Keywords Identification, Frequency Response, Transfer Functions, Multi–Input Multi–Output, Multivariate Statistics, Railway Comfort

1 Introduction

The vibrations significant for the comfort of the passengers of the trains are the total vibration and its components (vertical, longitudinal and lateral components) [1]. The measurements included linear accelerations on the x– y– and z–axis (Fig.1). Mechanical vibrations acted at the same time according to the x–, y–, and z– axis [2]. The accelerations acquired on the seat base and the seat–occupant interface of the train influenced the comfort of train passengers [3]. Passenger comfort can be assessed by the value of the vibration dose value (VDV) in time domain and by frequency response functions (FRFs) of the seat in frequency–domain. The knowledge of the VDV and FRFs on the seat–occupant interface allows the reduction of vibrations on the seat to improve the comfort of passengers [4].

Track irregularities generate multiaxis mechanical vibrations in a railway vehicle. The seat, headrests, and armrests represent a complex vibration environment. The accelerations acquired along the x– y– z-axis can be related to several sources of vibrations. Sources of vibration may be rigid motion, bending motion, torsional body motion of the railway vehicle, and vibratory motion generated by the dynamic interaction between wheel and track [5]. If the sources propagate vibratory signals according to x, y, and z directions, the rail-

way vehicle may be a multi–input, multi–output, and multiaxis mechanical system (Fig.2). The accelerations acquired on the seat along the x– y– z–axis, can be related linearly or not to the accelerations on the seat base along the x– y– z–axis [6].

A literature review evaluated that the single–input single–output (SISO) model does not detect seat vibrations in a complex vibration environment [7]. Researches have proposed multi–input multi–output (MIMO) and multi–input single–output (MISO) models, considering multiple vibration inputs on the seat base.

The modal properties and vibration transmission depend on the seat structure. Sitting on a train can be a single or double seat. In addition to the single–unit seat and the double–unit seat, another parameter is the number of seated subjects [8]. This research considered the single–unit seat and only one seated person. A prediction model evaluated the frequency response functions on a seat. The measurements of accelerations on the seat estimate railway comfort in time and frequency domain [9].

The assessment of comfort depends on human perception of vibrations, according to physical factors (amplitude, duration, frequency range) and psychological factors (type of population, gender, age, level of expectation, level of awareness). Human perception is related to the frequency range of mechanical stresses. Exposure to vibrations with small amplitudes but over a wide period can lead to concentration problems. Short exposures to large vibrations can damage the muscles and internal organs [10].

Vibration perception in the frequency range from 1 to 10 Hz is proportional to the magnitude of the accelerations. The human perception of vibrations in the frequency range from 10 to 100 Hz is proportional to the speed of the oscillations. The limit of human vibration perception is 0.001 m/s^2 and increases to 0.1 mm/s^2 at 100 Hz. In terms of speed, the limit of perception shall be between 0.1 and 0.3 mm/s for the vibration frequency range 1 to 100 Hz. The human body can detect vibration amplitudes of 0.001 mm. People can be annoyed by oscillations of 0.2 mm amplitude at 5 Hz, without causing damage. The magnitude of accelerations is a general characteristic of human perception, but the human response to vibrations is subjective.

This research proposes the calculation of VDV and frequency response functions of the passenger seat according to the x– y– z-axis of seat base and on a passenger–seat interface by the MIMO model. The MIMO model and the statistical approach recognized the frequencies of the maximum peak and estimated the passenger comfort. The identification approach evaluated the natural damped frequencies and the anti–resonance frequencies of railway vehicles. An optimization algorithm minimized the difference between analytical $G_{ij}(\omega)$ and experimental $H_{ij}(\omega)$ frequency response functions and involved the stability of the estimated $G_{ij}(\omega)$ function. The multivariate analysis considered the calculation of partial coherence, the cross-correlation functions, and the Anderson–Darling test to investigate the relations between input and output accelerations.

Figure 1. Seat System

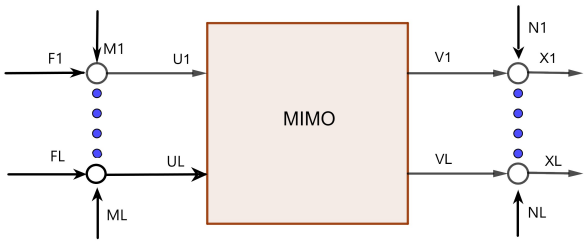

Figure 2. Multi–input Multi–Output Model

2 Mathematical and Statistical Analysis

A multi–input and multi–output model (MIMO), described in Table 1, evaluated the vibration transmission to a train seat. Firstly, the procedure estimated the vibration dose value in the time domain and maximum peaks in the frequency domain by an optimal identification of the transfer function. The cross–correlation functions evaluated the phase between input and output accelerations. Energy transfer from input to output characterized the MIMO model. The coherence functions estimated the energy transfer between input and output accelerations. Anderson–Darling test offered a test decision for the null hypothesis that the experimental data was from a population with a normal distribution.

2.1 Transfer Function of Multi–Input and Multi–Output Model

The input and output spectra can be represented, respectively, as $F_1(\omega)$, $F_2(\omega)$, ... , $F_P(\omega)$ and $X_1(\omega)$, $X_2(\omega)$, ..., $X_L(\omega)$ (Fig.2) for an MDOF railway vehicle with P input forces and L output responses. The spectra of input and output contain noise components. $M_1(\omega)$, $M_2(\omega)$, ..., $M_P(\omega)$ are the noise spectra from the input sides. $N_1(\omega)$, $N_2(\omega)$, ..., $N_L(\omega)$ are the noise spectra from the output sides. The noise free input and output spectra can be denoted as $U_1(\omega)$, $U_2(\omega)$, ..., $U_P(\omega)$ and $V_1(\omega)$, $V_2(\omega)$, ..., $V_L(\omega)$ respectively.

Step	Description
1	Define number m of inputs and number n of outputs
2	Assign input accelerations along x– y– and z–axis on the seat base
3	Assign output signal to train seat
4	Compute the vibration dose value in time domain
5	Identify maximum peaks in the frequency domain according to Eq.3 along x–, y– and z–axis of the seat by an optimal identification of the transfer function
6	Evaluate Anderson–Darling test
7	Develop Multiple Resolution Cross–Correlation Procedure
8	Compute autospectral and Cross–Spectral Density functions with the input and output accelerations
9	Compute the Partial and Multiple Coherency

Table 1. Algorithm for a multi–input and multi–output model

If the system presents noise, the output of the system at the ith coordinate is:

$$\begin{aligned} X_i(\omega) &= V_i(\omega) + N_i(\omega) \\ &= \sum_1^p H_{ij}(\omega)\left[F_j(\omega) - M_j(\omega)\right] + N_i(\omega) \\ &= \sum_1^p H_{ij}(\omega) F_j(\omega) + E_i(\omega) \end{aligned} \tag{1}$$

The symbol $E_i(\omega)$ represents the total measurement error in the system. Errors can be noise disturbances, signal processing, truncation. The accuracy of the FRF estimation depends on the error estimation. The transfer matrix becomes

$$G(\omega) = \begin{bmatrix} G_{11}(\omega) & G_{12}(\omega) & \dots & \dots & \dots & G_{1p}(\omega) \\ G_{21}(\omega) & G_{22}(\omega) & \dots & \dots & \dots & G_{2p}(\omega) \\ \vdots & \vdots & \dots & \dots & \dots & \vdots \\ G_{i1}(\omega) & G_{i2}(\omega) & \dots & G_{ij}(\omega) & \dots & G_{ip}(\omega) \\ \vdots & \vdots & & & & \vdots \\ G_{L1}(\omega) & G_{L2}(\omega) & \dots & \dots & \dots & G_{Lp}(\omega) \end{bmatrix} \tag{2}$$

where $G_{ij}(\omega)$ is the frequency response function for excitation at point i and response measurement at point i. For the multiple–input data acquisition method, the structure is excited with two or more exciters simultaneously.

The transfer function $G_{ij}(\omega)$ of any component of the transfer function matrix of MIMO system is expressed as ratio of two polynomials:

$$\begin{aligned} G_{ij}(\omega) &= \frac{N(\omega)}{D(\omega)} \\ &= \frac{C\left(\Omega_1^2 - \omega^2\right)\left(\Omega_2^2 - \omega^2\right)\dots\left(\Omega_m^2 - \omega^2\right)}{\left(\omega_1^2 - \omega^2\right)\left(\omega_2^2 - \omega^2\right)\dots\left(\omega_n^2 - \omega^2\right)} \end{aligned} \tag{3}$$

where

- ω_r $(r = 1, 2, \dots, n)$ are the natural damped frequencies;
- Ω_r $(r = 1, 2, \dots, m)$ are the anti–resonance frequencies;
- the reciprocal of constant C is the effective stiffness.

2.2 Optimal Identification of Transfer Function

The identification problem may be stated as the estimation of the natural damped frequencies and the anti–resonance frequencies of FRFs in such that difference between analytical $G_{ij}(\omega)$ (Eq.(3)) and experimental $H_{ij}(\omega)$ frequency response functions is minimized:

$$\begin{aligned} \min_{\omega_r, \Omega_r} \quad & \left|G_{ij}(\omega) - H_{ij}(\omega)\right| \\ \text{s.t.} \quad & \text{Hurwitz criterion} \end{aligned} \tag{4}$$

The optimization algorithm involves the stability of the estimated MIMO model:

Theorem 1 *In order to determine the existence of a root having a positive real part for a nth order polynomial with the positive coefficients can be used the algebraic criteria of stability: Hurwitz criterion. The Routh–Hurwitz stability criterion affirms that if all the principal minors of the Hurwitz matrix are positive and nonzero, a system with a characteristic equation of order n is asymptotically stable.*

The algorithm for checking the stability of the system in Eq.(3) can be summarized as the flow chart shown in Fig.3.

2.3 Multiple Resolution Cross–Correlation Procedure

The cross–correlation procedure proposes octave band alignment of the accelerations acquired on the floor and the seat according to the x, y, and z axes. Many tests validated the cross-correlation procedure. Cross-correlation shows similarity and dissimilarity between input and output. Cross–correlation showed that accelerations are not identical. Cross–correlation showed frequency shifts in octave bands. A lag value other than zero indicates frequency offset in the octave bands between input and output. A lag value of zero indicates zero offsets. If the phase shift is zero, the accelrations in octave bands are in phase. If the lag is different from zero, the accelerations in octave bands are not in phase.

The range of the cross–correlation function lies between (-1) and $(+1)$. A lag value 0 indicates that the two accelerations are correlated. A lag value 0 of cross-correlation indicates that the input and output are in phase. Anderson–Darling test, proposed in the following paragraph, assessed the source of the measurements.

2.4 Partial and multiple coherence functions

The coherence functions estimate the energy transferred from the inputs to the output. The coherence functions attribute to the energy ranking of the system. The calculation of

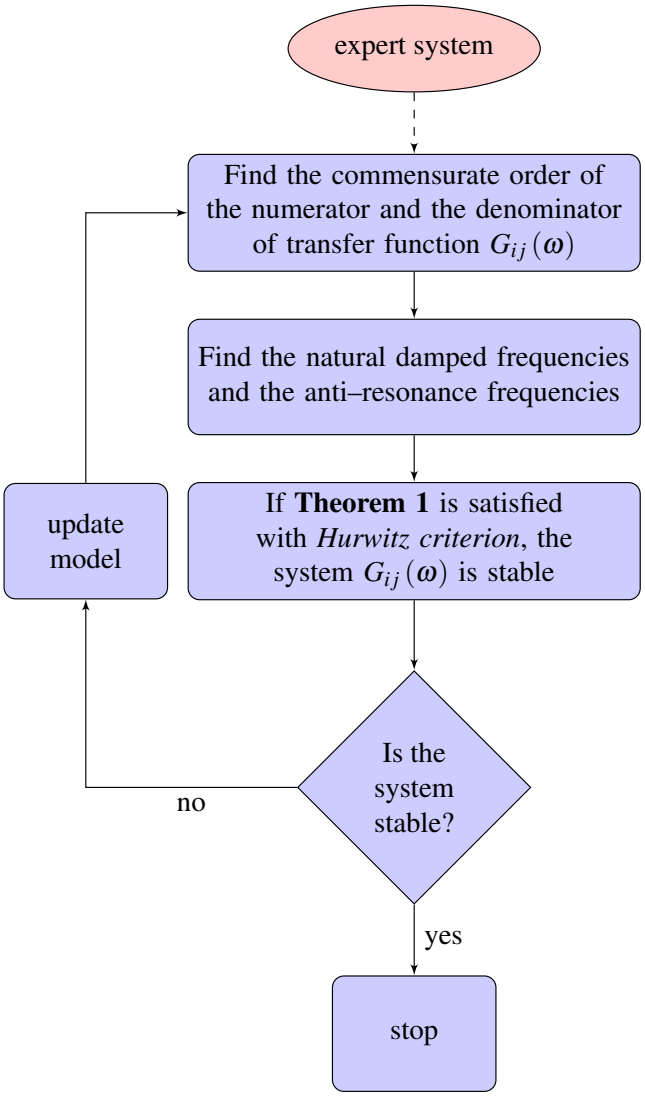

Figure 3. The algorithm for checking the stability of the mechanical system

the coherence function presents several factors. The measurement direction shall coincide with the axis of principal sensitivity of the accelerometer. Vibration sources can have a known or an unknown measuring point. The position of the measuring point influences the vibration measurements. The vibration sources can be or cannot be monitored directly. Vibration measurements are carried out on the vibration transmission path close to the inputs, resulting in contamination between energy sources.

2.5 Anderson–Darling test

Anderson–Darling (A–D) test estimates the provenance of the data sample from a population with a specific distribution. The A–D test is a modification of the Kolmogorov–Smirnov test (K–S). The A–D test was preferred to the K–S test because it gives more weight to the tails. The K–S test does not consider the type of distribution. The Anderson–Darling test uses a specific distribution in the calculation of critical values. The A–D test offered more sensitive investigations. By contrast, the A–D test has the disadvantage of calculating critical values for each distribution.

3 Results

3.1 Types of Trains

The High Frequentation Train (HFT) operates on regional routes of about 150–200 km. The HFT train reaches maximum speeds of about 130–160 km/h and an average speed of about 100 km/h. The HFT train stops about 1–2 minutes at each station, located between them at about 25-35 km. The power installed on the trains varies from 295 to 3500 kW. The HFT train uses a single vehicle or a composition of vehicles, up to a maximum of 5–6 elements. The use of one or more vehicles depends on the traffic flows of the line. Interregional trains have a higher power/mass ratio from 6.7 to 17.2 KW/t, allowing higher starting speeds and shorter average journey times. The number of passengers depends on the intensity of traffic. The HFT presents a minimum of 68 passengers for a single car to a maximum of 592 passengers for a convoy of 4–8 double-decker vehicles. HFT trains have functional and comfortable interiors but are not luxurious. The seats sitting are arranged every 1.5–2.5 meters. The interregional trains have functional and very comfortable interiors.

Four engines equipped the interregional electric trains (IET). The railway vehicle can reach a speed of 160 km/h. The trainset can be powered either at 1.5 or at 3 kV. The IET trains presented the low floor in the central part of the chests to allow a better ascent and descent of people and objects.

3.2 Vibration measurement method

All trains varied their speed during experimental investigations of mechanical vibrations. The seats consisted of a vertical backrest and a horizontal seat (Fig.1). A passenger sat in a comfortable upright posture with his back in contact with the backrest and his hands resting on his thighs. The Svantek multi–channel mechanical vibration analyzer SV 106A was equipped with three acceleration channels on the whole body. Acceleration acquisitions were implemented by ISO 2631. The vibrational comfort of the seats evaluated twenty experimental investigations on each train in the time and frequency domain. The duration of each measurement was 5 minutes. Octave analysis filters the signal and measures the energy at the input and output to provide frequency information

3.3 Time History Analysis

The time history analysis evaluated the dynamic response of trains to the excitation generated by the wheel–rail contact.

This section estimates the measured response using time domain data of the HFT (Fig.4), IET (Fig.5), Tramway (Fig. 6) and Underground (Fig.7).

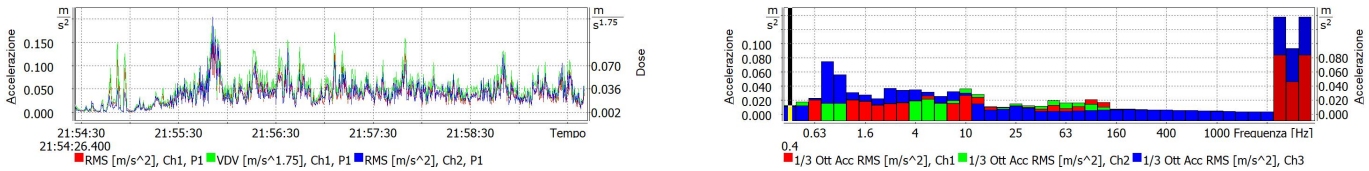

Figure 4. Time history and 1/3 Octave Analysis on High Frequentation Train along x– y– z–axis

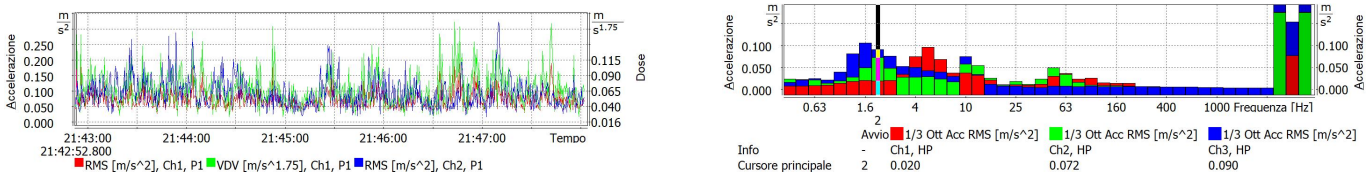

Figure 5. Time history and 1/3 Octave Analysis on Interregional Electric Train along x– y– z–axis

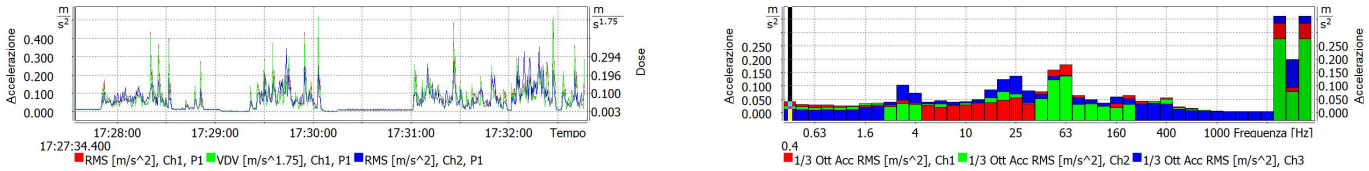

Figure 6. Time history and 1/3 Octave Analysis on Tramway along x– y– z–axis

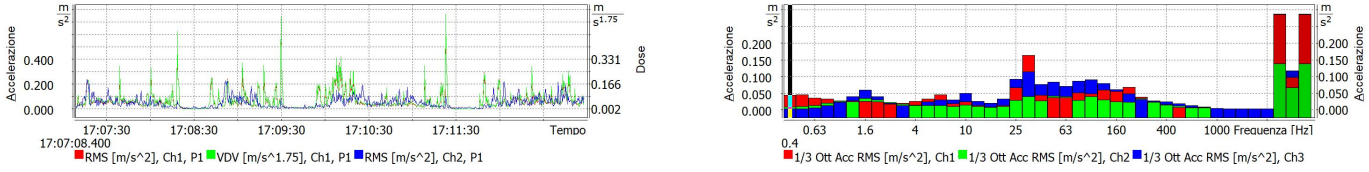

Figure 7. Time history and 1/3 Octave Analysis on Underground along x– y– z–axis

The time history analysis offers the values of peak [m/s^2], peak–peak [m/s^2],root mean square [m/s$^{1.75}$] and Vibration Dose Value (VDV) [m/s$^{1.75}$].The VDV has been analyzed according to x–, y–, and z–axis. The Figures 8 –11 propose the box and whisker plots of the VDV. The number of tests performed is 20 for each train. The dataset representation is summarized on five parameters: the minimum, the maximum, the sample median, and the first and third quartiles.

Time–domain data analysis showed that the worst axis was the z–axis for all trains. The median value of VDV, acquired on the high–frequency train according to z–axis, was 1.501 [m/s$^{1.75}$] (Fig.8). The median value of VDV, acquired on the interregional train according to z–axis, was equal to 0.7985 [m/s$^{1.75}$] (Fig.9). The median value of VDV, acquired on the Tramway according to z–axis, was 1.259 [m/s$^{1.75}$] (Fig.10). The median value of VDV, acquired on the Underground according to the z–axis, was equal to 0.7005 [m/s$^{1.75}$] (Fig.11).

The median values of the VDV, acquired on HFT, IET, Tramway and Underground according to the horizontal axes x and y, assumed values in the range 0.38–0.91 [m/s$^{1.75}$]. The median values of the VDV, according to the z–axis, were always greater than the median values according to the x– and y–axis on all trains.

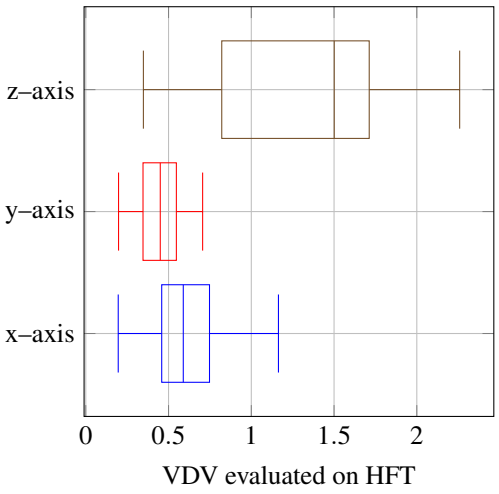

Figure 8. Box and whisker plots of Vibration Dose Value evaluated on High Frequentation Train

3.4 The Measurements of Multiple Resolution Cross–Correlation Procedure

Figures 12–15 propose the measurements of multiple resolution cross–correlation procedure.

The cross–correlation of the HFT showed lag=-1 between seat base and its seat along x–axis and z–axis. The lag became (+3) between the y–axis of the seat base and the y–axis of the seat. (Fig.12).

Cross–correlation functions of the IET presented lag=1 between the seat base x and seat x; the seat base y and seat y. The lag was (0) between the seat base z and the z–axis of the seat (Fig.13).

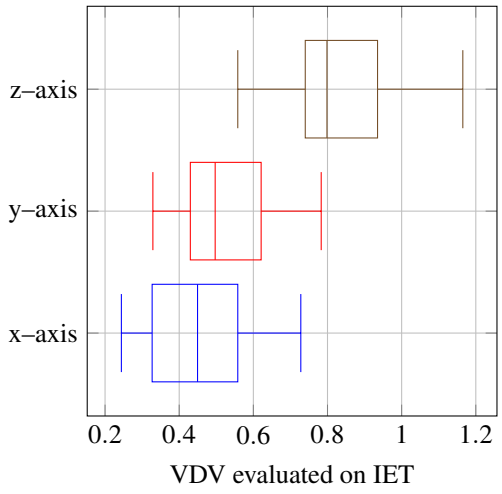

Figure 9. Box and whisker plots of Vibration Dose Value evaluated on Interregional Electric Train

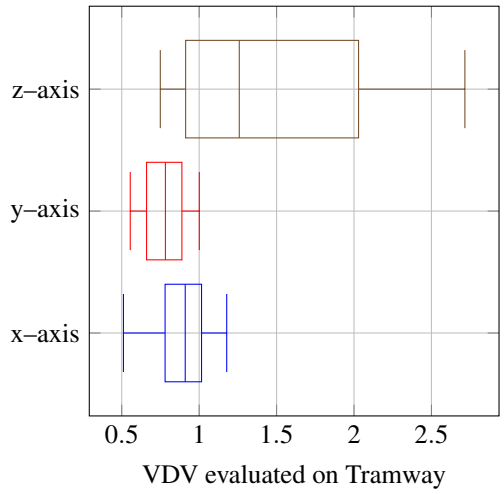

Figure 10. Box and whisker plots of Vibration Dose Value evaluated on Tramway

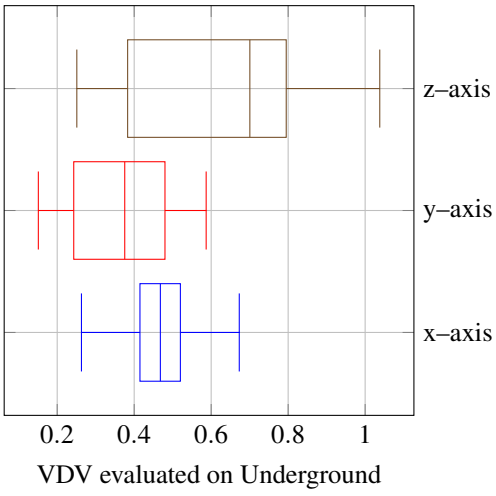

Figure 11. Box and whisker plots of Vibration Dose Value evaluated on Underground

Cross–correlation of the Tramway presented lag=-2 between the seat base x and seat x; the seat base z and seat z. The lag was (0) between the seat base y and the y–axis of the seat (Fig.14).

The cross–correlation of the Underground presented lag=0 between the seat base x and seat x; the seat base z and seat z. The lag was (+1) between the seat base y and seat y (Fig.15).

This examination illustrates that the phase changes between input and output accelerations in frequency domain. Input and output accelerations may be in phase, in advance or delayed between them.

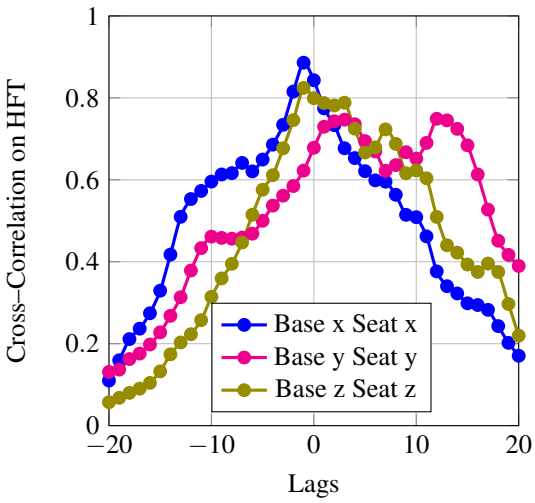

Figure 12. Cross–Correlation analysed on High Frequentation Train along Base x Seat x, Base y Seat y, Base z Seat y

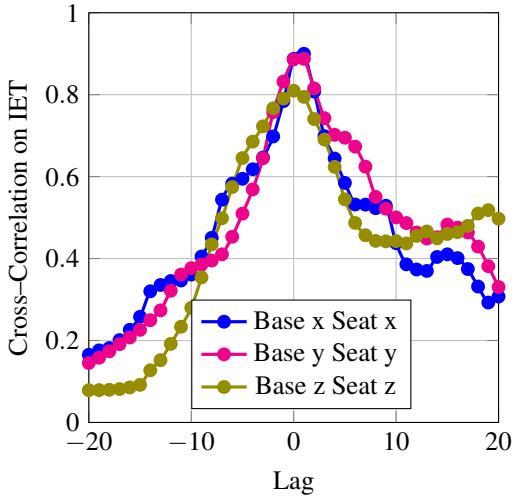

Figure 13. Cross–Correlation analysed on Interregional Electric Train along Base x Seat x, Base y Seat y, Base z Seat z

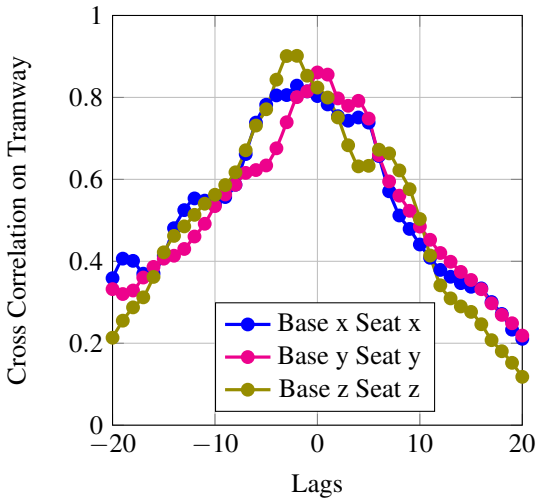

Figure 14. Cross–Correlation analysed on Tramway according to the measured accelerations: Base x Seat x, Base y Seat y, Base z Seat z

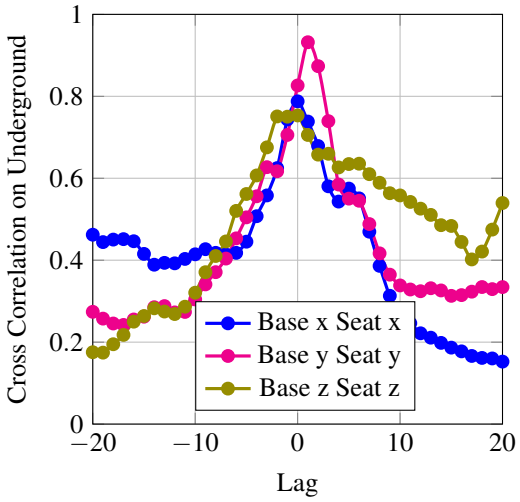

Figure 15. Cross–Correlation analysed on Underground Base x Seat x, Base y Seat y, Base z Seat z

3.5 The Measurements of the Coherence Functions

Figures 16–19 shows the measurements of coherence functions between inputs and output along the –x, –y, and –z axes

for all trains. The coherence functions showed a value of 0.9–1.0 in the frequency range 0–50 Hz for all trains.

A high value of the coherence functions is observed in the frequency range: 0–50 Hz. The high value of the coherence function indicated the high energy transfer from the inputs to the output.

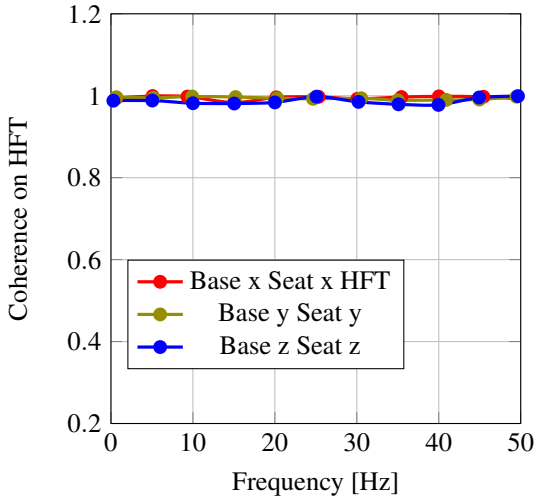

Figure 16. Coeherence evaluated on High Frequentation Train according to the measured accelerations: Base x Seat x, Base y Seat y, Floor z Seat z

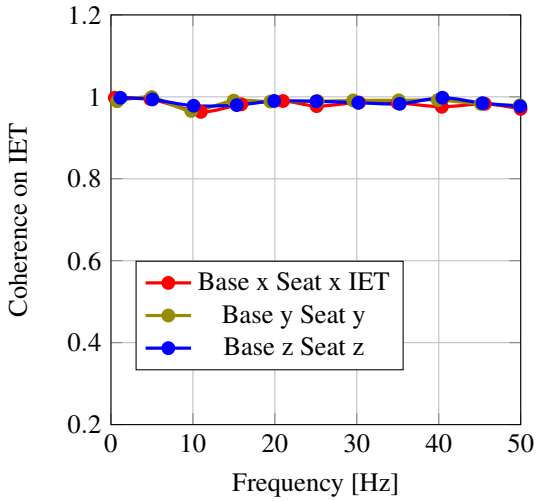

Figure 17. Coeherence evaluated on Interregional Electric Train according to the measured accelerations: Base x Seat x, Base y Seat y, Floor z Seat z

3.6 The Measurements of Anderson–Darling test

Anderson–Darling test returns a decision for the null hypothesis that the data is from a population with a normal distribution. The measurements return the p–value of the Anderson-Darling test; return the test statistic, A–D stat, and the critical value, CV, for the Anderson–Darling test. The returned value of $h = 0$ indicates that Anderson–Darling test fails to reject the null hypothesis at the default 5% significance level. For

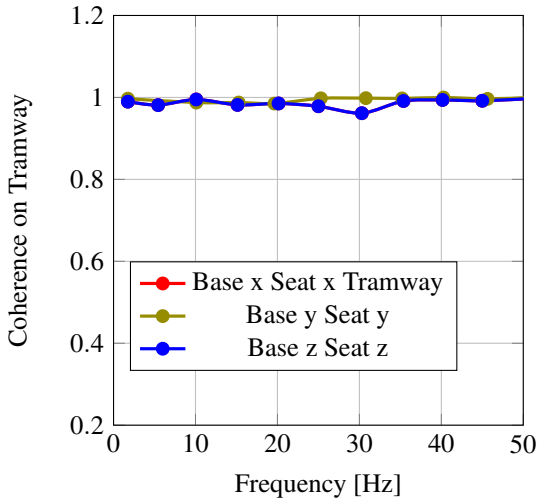

Figure 18. Coeherence evaluated on Tramway according to the measured accelerations: Base x Seat x, Base y Seat y, Floor z Seat z

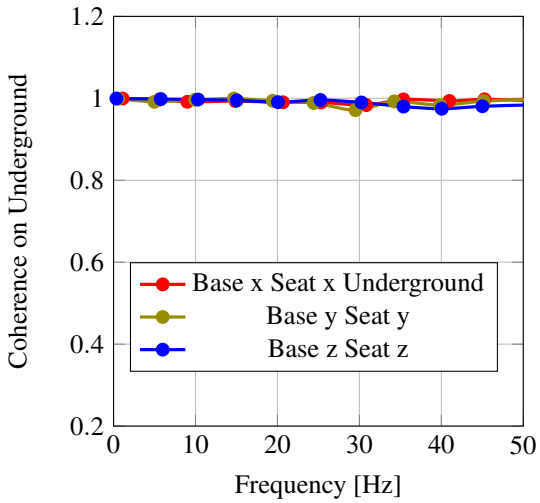

Figure 19. Coeherence evaluated on Underground according to the measured accelerations: Base x Seat x, Base y Seat y, Floor z Seat z

against, the returned value of $h = 1$ indicates that Anderson–Darling test rejects the null hypothesis at the default 5% significance level.

The experimental investigations showed the value $h = 1$. Therefore, the values of the accelerations came from different distributions (Table 2).

Train	h	p	AD stat	CV
IET	1	$5.0 \cdot 10^{-04}$	2.4254	0.7452
HFT	1	$5.0 \cdot 10^{-04}$	5.6282	0.7452
Underground	1	$5.0 \cdot 10^{-04}$	4.9288	0.7452
Tramway	1	$5.0 \cdot 10^{-04}$	5.7804	0.7452

Table 2. Anderson–Darling Test

3.7 Calibration of Mathematical Model by an Optimal Identification of Transfer Function

The dynamic of the railway vehicle depends on the contact of the wheel with the track and altimetric–planimetric features. The frequency response of the seat represented the passenger comfort in different conditions of motion: straight, curve, and braking. External forces resulted from the dynamic interaction between the wheel and the track. The variations in the altimetric and planimetric features imposed excitations on the railway vehicles. The braking and acceleration phases imposed excitations. The external forces of the railway vehicle developed the role-input of the railway vehicle. The output aspect included the assessment of various body regions: the feet, the interface seat-passenger, the back, shoulder/upper arm, wrist/hand, and neck.

The Eq.(3) offered an algorithm for the identification of response of passenger comfort in the frequency domain. The measuring points were on the seat base and the interface seat–passenger of the trains. The algorithm reached full convergence between the data obtained by the mathematical model Eq.(3) and the experimental results (Figures 20–23). The iterative algorithm minimized the error with the constraint that the MIMO model of the railway vehicle was stable.

3.8 1/3 Octave Band Analysis

The structures of the MIMO model are transfer functions, represented by Eq.(3). The identification approach estimates peaks by minimizing the error between the model output and the measured response. In addition, the identification approach performs residual analysis by the coefficient of determination R–squared between the model output and the measured response to assess the model quality. The experimental design considered twenty tests for each train. The range of variation of the R–squared was 0.95–1.0.

This section estimates the measured response using frequency domain data of the HFT (Fig.4), IET (Fig.5), Tramway

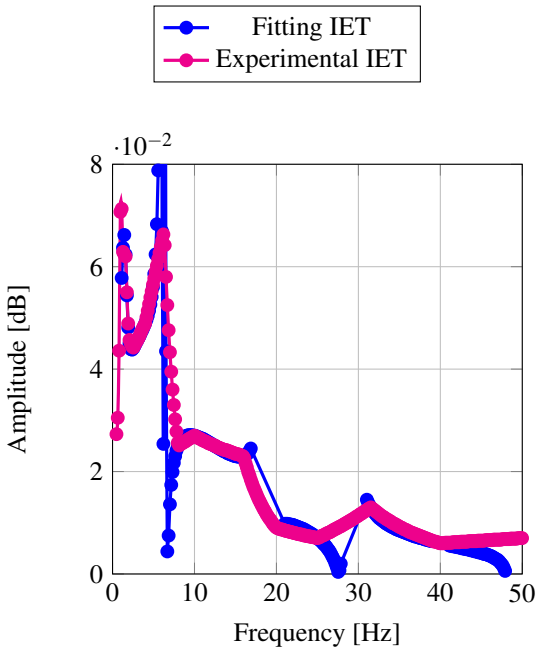

Figure 20. Comparison between estimated and experimental FRFs along z–axis on Interregional Electric Train

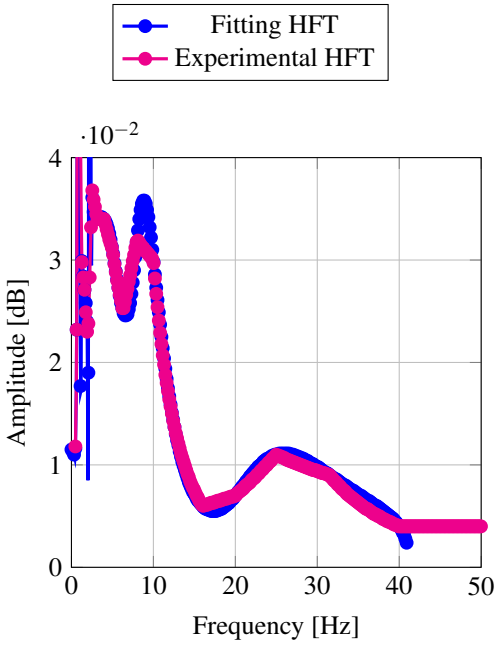

Figure 21. Comparison between estimated and experimental FRFs along z–axis on High Frequentation Train

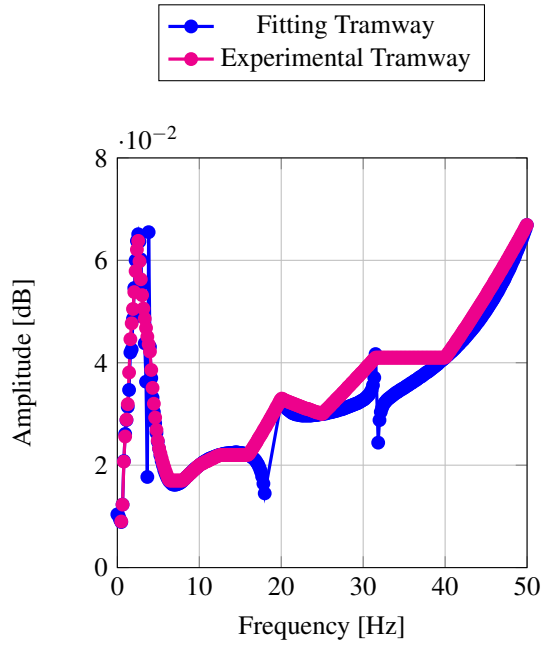

Figure 22. Comparison between estimated and experimental FRFs along z–axis on Tramway

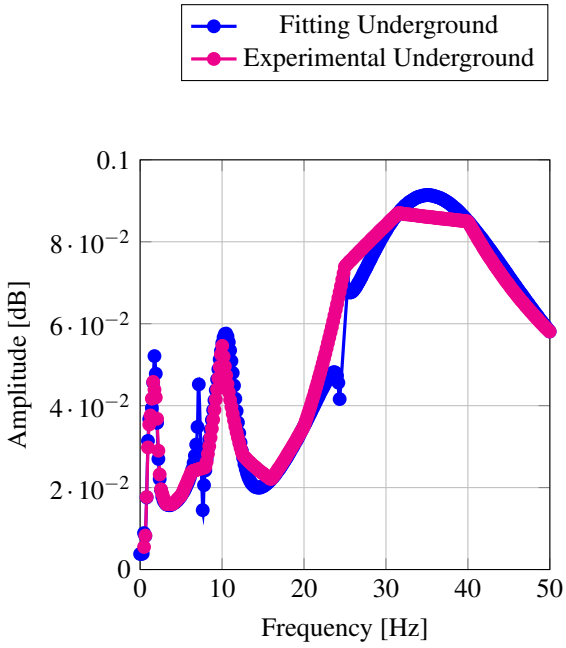

Figure 23. Comparison between estimated and experimental FRFs along z–axis on Underground

(Fig. 6) and Underground (Fig.7).

The 1/3 Octave Band on HFT showed three peaks according to the x, y, and z axes. Generally speaking, the position of the first peak depends on the axis of vibrations. According to the x-axis, the first peak was at about 3.15 Hz, the second peak was at 10 Hz, and the third peak was at 25 Hz. The first peak was at about 2.5 Hz, the second peak was at about 10 Hz, and the third peak was at 25 Hz according to the y–axis and the z–axis.

The 1/3 Octave Band on IET showed that the number of peaks depends on the axis of vibration. The peaks were two along the x-axis. The first peak was at about 1.6 Hz the second peak was at about 6.3 Hz. According to the y-axis, the first peak was at about 1.6 Hz, the second peak was at 5 Hz, and the third peak was at 12.5 Hz. The first peak was at 1.6 Hz, the second peak was at 6.3 Hz, and the third peak was at 10 Hz along the z–axis.

The 1/3 Octave Band on Tramway showed similar values between the x and y axes. According to the x–axis, experimental tests showed two peaks at about 3.15 Hz and 16 Hz. The tests have shown, in addition to predicted peaks, the third peak at 31.5 Hz. According to the vertical axis, the peaks were at 3.15, 12.5, and 25 Hz.

The 1/3 Octave Band on Underground pointed out that the x–axis was under little stress. The experimental tests showed only one peak at 8 Hz according to the x–axis. According to the y–axis, the peaks were at 1.6, 10, and 25 Hz. According to the z–axis, the maximum values were at 1.25, 10, and 16 Hz.

A rigid train mode caused the first peak. The second peak may be related to the flexible vibration modes of the train. The third peak may be related to the forced excitation generated by the external forces acting on the railway vehicle.

Train	Axis	1st	2nd	3rd
		Hz		
HFT	x	2.5	10.0	25.0
	y	3.15	10.0	25.0
	z	2.5	10.0	25.0
IET	x	1.6	6.3	–
	y	1.6	5.0	12.5
	z	1.6	6.3	10.0
Tramway	x	3.15	16	–
	y	3.15	16.0	31.5
	z	3.15	12.5	25.0
Underground	x	8.0	–	–
	y	1.6	10.0	25.0
	z	1.25	10.0	16.0

Table 3. 1/3 Octave Band Frequencies

4 Discussion

The acceleration spectra along the x–axis of the seat are distributed mainly over the frequency range 0–25 Hz with a characteristic peak at about 2.5, 3.15, and 8.0 Hz concerning the type of train (Table 3).

The acceleration spectra along the y–axis of the seat are distributed mainly over the frequency range 0–30 Hz with a characteristic peak at about 1.6, 3.15 Hz concerning the type of train (Table 3).

The acceleration spectra according to the z–axis of the seat are distributed mainly over the frequency range 0–25 Hz with a characteristic peak at about 1.25, 1.6, 2.5, and 3.15 Hz concerning the type of train (Table 3).

The acceleration spectra according to the z–axis direction of the seat are distributed mainly over the frequency range 0–25 Hz with characteristic vertical oscillations caused by the line altitude discontinuities. Track irregularities caused lateral and transverse vibrations. The lateral displacement of the wheels of a railway vehicle moving on the line triggered the motions of the railway axles.

The transfer function $G_{ij}(s)$ of the MIMO system depends on the modal properties of the mechanical systems. The transfer functions $G_{ij}(s)$ depend on natural frequencies and damping ratio. The mathematical approach evaluated partial coherence functions between input and output accelerations along the x– y– z–axis. Transfer functions showed the peak frequencies by the peak picking method. The following hypotheses are assumed: each significant peak in the frequency–response functions corresponds exactly to a vibrational mode; the system corresponds to a damped harmonic oscillator of a degree of freedom close to the maximum value of FRF. Experimental investigations showed that the peak frequencies depend on the type of train and the axis examined. The first peak was at 2–3 Hz, generated by the rigid vibration mode of the train. The second peak was at 10–16 Hz, corresponding to a flexible vibration mode, and the third peak was at 25–30 Hz, which may result from forced vibration induced by dynamic interaction between wheel and track of railway vehicles.

The Figure 16–19 represents the coherence between the accelerations according to the three axes. The coherence between input and output accelerations was close to 0.9–1.0, indicating that the system assumes a linear behavior according to the three directions. The coherence functions justified the adoption of a multi–input multi–output model.

Tram, light rail, and train systems are urban and suburban means of transport in many European cities. The passenger onboard can be exposed to vibration, noise, and temperature. The service quality indices offered to the passengers concern the monitoring, respectively, of the quality of comfort in tramway vehicles and driving quality. The subjective sense of the passengers exposed to vibrations influences the judgment on the quality of driving and comfort in tramway vehicles. The assessment of the quality of running comfort shall examine the accelerations recorded on the seat.

Rail tracks of light rail vehicles, such as trams, differ from rail tracks. The running surface of rail tracks of light rail vehicles is shared with road vehicles. Therefore, travel on light rail vehicles differs from travel on standard train vehicles. The tram trip can be a fast connection to the city without stops; it can be a slow start–stop the ride in a traffic situation in the presence of other road vehicles; it can be a journey on a path with narrow and winding curves. The calculation of VDV, frequency analysis, and statistical survey can guide to improve the running comfort of passengers.

The ballast characterizes the railway lines and affects the comfort. The ballast is a construction composed of rubble, stones, or other incoherent material used as a support base for railway infrastructure. The tramway track structure is different from the railway roadbed. The classic track is ballasted. The tramway track structure uses grooved rails. The base consists of continuous concrete slabs. The road contains the runway of the rolling surface. The groove is shallow at the crossroads. The tram runs on tracks embedded in the road. The tramway runs on stretches with its headquarters, in tunnels, and on the elevated road to improve circulation. Therefore, the tramway runs on different types of roads.

Another aspect is the speed of the train. Vehicles on standard tracks operate at speeds and travel longer distances than vehicles on the tramway network. The journey by train presents the following aspects: medium/long distances between stops; medium/high speed; gentle curvature of the track according to the track layout. On the other hand, tramway travel presents the following aspects: short distances between tram stops; low speed; complex track curvature according to the route of city roads; mixed road/rail traffic along the route.

5 Conclusions

A multi–input multi–output (MIMO) model of railway comfort considered vehicles operating, respectively, on railway tracks standard and the tramway. The multivariate analysis estimates measurements based on accelerations to capture the complexity between inputs and outputs according to the x– y– z–axis. The MIMO model identified the maximum acceleration amplitude values in the frequency domain and assessed rail comfort. The MIMO model evaluated the transmissibility of the system passenger seat exposed to lateral and vertical vibrations by the partial coherence functions, the cross–correlation functions, and the Anderson–Darling nonparametric test. The mathematical and statistical analysis evaluated the contribution of every single input to the response (output). The results showed that the peak frequencies depend on the type of train and the axis examined. The first peak was at 2–3 Hz, generated by the rigid vibration mode of the train. The second peak was at 10–16 Hz, corresponding to a flexible vibration mode, and the third peak was at 25–30 Hz, which may result from forced vibration induced by the dynamic interaction between wheel and track of railway vehicles.

Railway comfort examined transport requirements concerning vibration exposure, vehicle type, number of journeys, passengers, and personnel involved at the service.

The passenger qualified the quality of the vehicle according to his feelings. Vibration data acquired on railway vehicles can assess passenger comfort and infrastructure performance. The dynamic interaction between wheel and track depends on the

velocity of the trains, track geometry, characteristics such as alignment, track defects (soldering, deformations, rail breaks, track geometry), and the overhead line. Future developments concern the evaluation of lateral and vertical comfort indices to estimate the effect of train speeds, changes in altitude, and curves of railway lines. The MIMO model predicts future response values of the whole human body in railway vehicles.

HFT	High Frequentation Train
IET	Interregional Electric Train
h	Hypothesis test result $1\|0$
p	p–value (scalar value) in the range $[0,1]$
AD stat	Test statistic
CV	Critical Value
$E_i(\omega)$	total measurement error
$G_{ij}(s)$	estimated transfer functions
$H_{ij}(s)$	experimental transfer functions
ω_r	natural damped frequencies
Ω_r	anti–resonance frequencies

Table 4. List of Symbols

Conflict of interest

The Author declares that he has no conflict of interest.

REFERENCES

[1] Graa M, Nejlaoui M, Houidi A, Affi Z, Romdhane L, Modeling and Simulation for Vertical Rail Vehicle Dynamic Vibration with Comfort Evaluation. In: Haddar M. et al. (eds) Multiphysics Modelling and Simulation for Systems Design and Monitoring. MMSSD 2014. Applied Condition Monitoring, vol 2. Springer, 2015. https://doi.org/10.1007/978-3-319-14532-7-6.

[2] Cavacece M, Aghilone G, Optimisation of the contact damping and stiffness coefficients to attenuate vertical whole–body vibration. 6th Internaltional Conference on Whole–Body Vibration Injuries, June 19–21, 93, 2017, ISBN 978–91–85971–64–0, ISSN 0346–7821.

[3] Cavacece M, Aghilone G, Intra–subject Variability of Impact Shock of Foot on the Ground during Walking and Running Activities, Universal Journal of Public Health, 6(4), 167–172,2018. DOI: 10.13189/ujph.2018.060401

[4] Dumitriu M,Mihai L, Correlation between Ride Comfort Index and Sperling's Index for Evaluation Ride Comfort in Railway Vehicles. Applied Mechanics and Materials, 880, 201–206, 2018. https://doi.org/10.4028/www.scientific.net/AMM.880.201

[5] Haladin I, Lakušić S, Bogut M, Overview and analysis of methods for assessing ride comfort on tram tracks. Gradevinar, 71, 10, 901–921, 2019.DOI: https://doi.org/10.14256/JCE.2731.2019

[6] Yanran Jianga, Chena B K., Cameron T, A comparison study of ride comfort indices between Sperling's method and EN 12299.International Journal of Rail Transportation,7(4), 279–296, 2019.https://doi.org/10.1080/23248378.2019.1616329.

[7] Wu J, Qiu Y, The study of seat vibration transmission of a high–speed train based on an improved MISO method. Mechanical Systems and Signal Processing, 143, 106844, 1–20, 2020, https://doi.org/10.1016/j.ymssp.2020.106844

[8] Sadeghi J, Rabieea S, Khajehdezfuly A, Development of train ride comfort prediction model for railway slab track system. Latin American Journal of Solids and Structures,17(7), 304, 2020.https://doi.org/10.1590/1679-78256237.

[9] Zboinski Krzysztof, Woznica Piotr, Optimum Railway Transition Curves–Method of the Assessment and Results,Energies, 14(13), 3995, 2021. https://www.mdpi.com/1996-1073/14/13/3995.

[10] Dumitriu M, Stănică D I, Study on the Evaluation Methods of the Vertical Ride Comfort of Railway Vehicle–Mean Comfort Method and Sperling's Method. Applied Science 2021, 11(9), 3953, 3953, 1–25,2021,https://www.mdpi.com/2076-3417/11/9/3953.